Inorg. Chem. **2008**, *47*, 4413−4420

Why Does Cyanide Pretend to be a Weak Field Ligand in $[Cr(CN)_5]^{3-}$?

Richard L. Lord and Mu-Hyun Baik*

Department of Chemistry and School of Informatics, Indiana University, Bloomington, Indiana 47405

Received January 13, 2008

Chemical reasoning based on ligand-field theory suggests that homoleptic cyano complexes should exhibit low-spin configurations, particularly when the coordination sphere is nearly saturated. Recently, the well-known chromium hexacyano complex anion $[Cr(CN)_6]^{4-}$ was shown to lose cyanide to afford $[Cr(CN)_5]^{3-}$ in the absence of coordinating cations. Furthermore, $(NEt_4)_3[Cr(CN)_5]$ was found to be in a high-spin ($S = 2$) ground state, which challenges the common notion that cyanide is a strong field ligand and should always enforce low-spin configurations. Using density functional theory coupled to a continuum solvation model, we examined both the instability of the hexacyanochromate(II) anion and the relative energies of the different spin states of the pentacyanochromate(II) anion. By making direct comparisons to the analogous Fe^{II} complex, we found that cyanide electronically behaves as a strong-field ligand for both metals because the orbital interaction is energetically more favorable in the low-spin configuration than in the corresponding high-spin configuration. The Coulombic repulsion between the anionic cyanide ligands, however, dominates the overall energetics and ultimately gives preference to the high-spin complex, where the ligand−ligand separation is larger. Our calculations highlight that for a quantitative understanding of spin-state energetic ordering in a transition metal complex, ligand−ligand electrostatic interactions must be taken into account in addition to classical ligand−field arguments based on M−L orbital interaction energies.

Introduction

A key characteristic of transition metal complexes is their ability to adopt different spin states as a function of the ligand environment.[1,2] In particular, first-row metals with four to seven d-electrons exhibit great flexibility in adopting high- or low-spin configurations.[1] The relationship between orbital energy splitting (Δ_o) and electron pairing energies that ultimately determine which spin state is adopted is conceptually well understood.[2] Predictions beyond qualitative trend analyses, for example, using Tanabe−Sugano diagrams,[3,4] are difficult. Most useful for a practical application of ligand field theory is the spectrochemical series[2] that provides a convenient empirical scale for the strength of the ligand field associated with a specific ligand. It identifies cyanide and carbon monoxide, both displaying strong σ-base and π-acid characteristics, as two of the best strong-field ligands available in the toolbox of an organometallic chemist. Hence, the Cr^{II}-d^4-center of the homoleptic cyano complex $[Cr(CN)_6]^{4-}$ is a textbook example of a weakly Jahn−Teller distorted octahedral low-spin ($S = 1$) complex, and it is not surprising that $K_4[Cr(CN)_6]$ displays magnetic properties that are most consistent with a $S = 1$ spin configuration.[5]

Remarkably, Nelson et al. found recently that $[Cr(CN)_6]^{4-}$ is structurally unstable if noncoordinating cations, such as $(NEt_4)^+$, are used during synthesis. Instead of the expected tetraanionic complex, the trianionic $[Cr(CN)_5]^{3-}$ complex was isolated.[6] Magnetic susceptibility measurements revealed that the $[Cr(CN)_5]^{3-}$ ion is a high-spin complex ($S = 2$), which raises some fundamental questions. First, the apparently weak ligand field giving rise to the high-spin $[Cr(CN)_5]^{3-}$ ion is puzzling and challenges the simplistic classification of cyanide as a strong field ligand. Second, the observed structural instability of the $[Cr(CN)_6]^{4-}$ ion is difficult to understand because the analogous $[Fe(CN)_6]^{4-}$ anion is not only stable in the absence of coordinating cations but also displays relatively short M−CN bonds of 1.90−1.94 Å.[7−15] A recent

* To whom correspondence should be addressed. E-mail: mbaik@indiana.edu.

(1) Gütlich, P.; Goodwin, H. A. *Spin Crossover in Transition Metal Compounds*; Springer: Berlin, 2004.
(2) Cotton, F. A.; Murillo, C. A.; Bochmann, M. *Advanced Inorganic Chemistry*; Wiley: New York, 1999.
(3) Tanabe, Y.; Sugano, S. *J. Phys. Soc. Jpn.* **1954**, *9*, 753–766.
(4) Tanabe, Y.; Sugano, S. *J. Phys. Soc. Jpn.* **1954**, *9*, 766–779.
(5) Eaton, J. P.; Nicholls, D. *Transition Met. Chem.* **1981**, *6*, 203–206.
(6) Nelson, K. J.; Giles, I. D.; Shum, W. W.; Arif, A. M.; Miller, J. S. *Angew. Chem., Int. Ed.* **2005**, *44*, 3129–3132.
(7) Meyer, H.-J.; Pickardt, J. *Acta Crystallogr. C* **1988**, *44*, 1715–1717.
(8) Razak, I. A.; Shanmuga Sundara, R. S.; Fun, H.-K.; Tong, Y.-X.; Lu, Z.-L.; Kang, B.-S. *Acta Crystallogr. C* **2000**, *56*, 291–292.
(9) Soria, D. B.; Piro, O. E.; Varetti, E. L.; Aymonino, P. J. *J. Chem. Crystallog.* **2001**, *31*, 471–477.

10.1021/ic8000653 CCC: $40.75
Published on Web 04/23/2008

theoretical report[16] provided a formal protocol for interpretation of this curious observation in the ligand-field theory framework, but an intuitive, conceptual understanding of the features that govern the relative stabilities of homoleptic chromium(II) complexes is thus far not available. We used density functional methods,[17,18] coupled to a continuum solvation model,[19] to construct a model that reproduces the experimental observations, which is then analyzed in detail to identify the electronic features that give rise to the unclassical energetic ordering of the different spin states. To better understand what makes the chromium complex so special, we compared the Cr^{II} complex to its Fe^{II} analogue that displays classical spin-state energies. Our results suggest that the unclassical behavior of the $[Cr(CN)_5]^{3-}$ complex can be rationalized with classical arguments, namely, by considering ligand-field strength as a function of M−L distances, as well as the associated Coulombic forces.

Computational Details

All calculations were carried out using density functional theory (DFT) as implemented in the Amsterdam Density Functional Package, version 2005.01.[20] Unrelated previous studies have shown that prediction of the relative energies of different spin states of transition metal complexes with DFT can be difficult.[21−23] Whereas DFT has been very successful for many applications, serious problems are encountered when popular exchange-correlation functionals, such as the widely used B3LYP functional,[24,25] are used to model the relative energies of different spin states. The main problem with hybrid functionals is that the exchange potential, which is only nonzero for parallel-spin electrons, is too attractive giving rise to exaggerated stabilization of high-spin states compared to their low-spin analogues. On the other hand, pure functionals which have no explicit Hartree−Fock exchange component tend to favor low-spin configurations. Because all of our arguments presented here revolve about the accessibility of the high-spin states, we have chosen to use the BLYP functional recognizing that the computed energies of the high-spin states are likely too high and the true preference of the high-spin states is likely more dramatic than discussed below.

Geometry optimizations were performed with the TZ2P basis set in ADF, based on Slater-type orbitals, which is a triple-ζ basis with two sets of additional polarization functions.[26] Relativistic effects on Cr and Fe were included using the zero-order relativistic approximation (ZORA).[27,28] These geometries were confirmed to be minima on the potential energy surface by running frequency calculations at each equilibrium structure and ensuring there were no imaginary frequencies. Unscaled harmonic frequencies were used to derive the entropy and zero-point energy (ZPE) corrections. Note that by entropy here we refer to the entropy of the solute alone. As is common in all continuum solvation models, the entropy changes of the solvents are included implicitly. Solvation energies were computed at the optimized gas-phase structures using the COSMO method,[19,29] with a dielectric constant of 37.5 for acetonitrile. The atomic radii used were as follows: C, 2.30 Å; H, 1.16 Å; N, 1.40 Å; Cr, 1.39 Å; Fe, 2.40 Å. Acetonitrile was chosen to match the experimental work by Nelson et al.[6] The solvent-excluding surface was used to construct the solute cavity with a probe radius set to 1.4 Å. Thermodynamic properties were calculated as follows (eqs 1−3)

$$\Delta H(\text{gas}) = \Delta E(\text{bond}) + \Delta ZPE \quad (1)$$

$$\Delta G(\text{gas}) = \Delta H(\text{gas}) - T\Delta S(\text{gas}) \quad (2)$$

$$\Delta G(\text{sol}) = \Delta G(\text{gas}) + \Delta G_{\text{solv}} \quad (3)$$

To gain a deeper understanding of the metal−ligand bonding in these complexes, the energy decomposition introduced by Ziegler and Rauk has been employed.[30,31] In the Ziegler−Rauk decomposition scheme, the binding energy between two molecular fragments (ΔE_{bind}) is divided into the preparation energy (ΔE_{prep}), that is, the energy associated with distorting the fragment equilibrium geometries to their preassembled complex geometries in the absence of the other fragment, and an interaction energy (ΔE_{int}) between these prepared fragments (eq 4). This interaction energy is further decomposed into three components (eq 5): the Pauli repulsion energy (ΔE_{Pauli}), the electrostatic interactions ($\Delta E_{\text{electrostatic}}$), and the orbital interactions (ΔE_{oi}). Initially, when the fragments are brought together, the electron density of each individual fragment is not allowed to relax. The penalty resulting from the antisymmetry requirement of the electrons gives rise to the Pauli repulsion energy. The electrostatic interactions are the classical attractions and repulsions arising from the Coulombic forces between electron densitites and the nuclei. Finally, the orbital interactions describe the energy gained upon letting the orbitals of this "supermolecule" relax. A more detailed discussion about the individual components and the implementation in ADF can be found in ref 31.

$$\Delta E_{\text{bind}} = \Delta E_{\text{prep}} + \Delta E_{\text{int}} \quad (4)$$

$$\Delta E_{\text{int}} = \Delta E_{\text{Pauli}} + \Delta E_{\text{electrostatic}} + \Delta E_{\text{oi}} \quad (5)$$

Results and Discussion

In general, there are three spin states to consider for a Cr^{II}-d^4-ion in an octahedral coordination environment. All four metal-based valence electrons can occupy different spatial MOs to afford the *high-spin* ($S = 2$) state. Alternatively, two valence electrons may occupy the same MO, giving rise to the $S = 1$ configuration. Finally, all electrons

(10) Antipin, M. Y.; Ilyukhin, A. B.; Kotov, V. Y. *Mendeleev Commun.* **2001**, 210–211.
(11) Antipin, M. Y.; Ilyukhin, A. B.; Kotov, V. Y.; Lokshin, B. V.; Seifer, G. B.; Chuvaev, V. F.; Yaroslavtsev, A. B. *Russ. J. Inorg. Chem.* **2002**, *47*, 1031–1037.
(12) Ferlay, S.; Bulach, V.; Felix, O.; Hosseini, M. W.; Planeix, J. M.; Kyritsakas, N. *CrystEngComm* **2002**, 447–453.
(13) Kotov, V. Y.; Ilyukhin, A. B. *Mendeleev Commun.* **2003**, 169–170.
(14) Malarova, M.; Kuchar, J.; Cernak, J.; Massa, W. *Acta Crystallogr. C* **2003**, *59*, M280−M282.
(15) Bie, H. Y.; Lu, J.; Yu, J. H.; Sun, Y. H.; Zhang, X.; Xu, J. Q.; Pan, L. Y.; Yang, Q. X. *J. Coord. Chem.* **2004**, *57*, 1603–1609.
(16) Deeth, R. J. *Eur. J. Inorg. Chem.* **2006**, 2551–2555.
(17) Parr, R. G.; Yang, W. *Density Functional Theory of Atoms and Molecules*; Oxford University Press: New York, 1989.
(18) Baerends, E. J.; Gritsenko, O. V. *J. Phys. Chem. A* **1997**, *101*, 5383–5403.
(19) Klamt, A.; Schüürmann, G. *J. Chem. Soc., Perkin Trans. 2* **1993**, 799–805.
(20) *Amsterdam Density Functional*, version 2005.01; Vrije Universiteit Amsterdam: Amsterdam, The Netherlands, 2005.
(21) Reiher, M.; Salomon, O.; Hess, B. A. *Theor. Chem. Acc.* **2001**, *107*, 48–55.
(22) Salomon, O.; Reiher, M.; Hess, B. A. *J. Chem. Phys.* **2002**, *117*, 4729–4737.
(23) Swart, M.; Groenhof, A. R.; Ehlers, A. W.; Lammertsma, K. *J. Phys. Chem. A* **2004**, *108*, 5479–5483.
(24) Becke, A. D. *J. Chem. Phys.* **1993**, *98*, 5648–5652.
(25) Lee, C. T.; Yang, W. T.; Parr, R. G. *Phys. Rev. B* **1988**, *37*, 785–789.
(26) Van Lenthe, E.; E, J. B. *J. Comput. Chem.* **2003**, *24*, 1142–1156.
(27) van Lenthe, E.; van Leeuwen, R.; Baerends, E. J.; Snijders, J. G. *Int. J. Quantum Chem.* **1996**, *57*, 281–293.
(28) van Lenthe, E.; Baerends, E. J.; Snijders, J. G. *J. Chem. Phys.* **1993**, *99*, 4597–4610.
(29) Pye, C. C.; Ziegler, T. *Theor. Chem. Acc.* **1999**, *101*, 396–408.

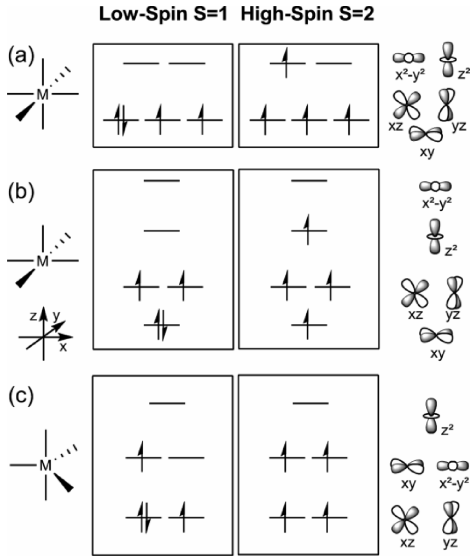

Figure 1. Idealized MO diagrams for octahedral, square pyramidal, and trigonal bipyramidal coordination geometries, respectively.

may be paired to give the $S = 0$ state. Not surprisingly, the $S = 0$ state was consistently found to be >20 kcal mol^{-1} higher in energy than the $S = 1$ state, disqualifying it from further consideration. Therefore, *low-spin* refers to the $S = 1$ configuration throughout this study. Whereas a weakly Jahn−Teller distorted octahedral coordination geometry is most reasonable for $[Cr(CN)_6]^{4-}$, both square-pyramidal and trigonal-bipyramidal structures are plausible for $[Cr(CN)_5]^{3-}$. Conceptual MO diagrams for these structural motifs are illustrated in Figure 1.[32] Interestingly, our calculations indicate that the intuitively expected, "naked" low-spin $[Cr(CN)_6]^{4-}$ ion is a proper minimum on the potential energy surface, which was not detected experimentally. When the high-spin configuration for $[Cr(CN)_6]^{4-}$ is enforced, however, at least one cyanide ligand is lost during geometry optimization, which can be understood easily by realizing that either the d_{z^2} or $d_{x^2-y^2}$ orbital that is empty in the low-spin state becomes occupied in the hypothetical high-spin state (Figure 1a). Because these MOs are strongly M−L antibonding, their occupation results in loss of a ligand. Thus, we were unable to locate a proper structure for the high-spin $[Cr(CN)_6]^{4-}$ ion. For pentacyanochromate(II), on the other hand, the high-spin state is energetically favored by ∼12 kcal mol^{-1} over the expected low-spin state, where the trigonal bipyramidal structure was found to be 1.5 kcal mol^{-1} lower in energy than the square-pyramidal analogue, in line with the observation that the square pyramidal and trigonal bipyramidal structures cocrystallize. Our results suggest that they should also coexist in the solution phase. The computed geometries of the low-spin $[Cr(CN)_6]^{4-}$ ion and two structural isomers of the high-spin $[Cr(CN)_5]^{3-}$ complex are shown in Figure 2. The metal−cyanide bond lengths of the Jahn−Teller distorted low-spin $[Cr(CN)_6]^{4-}$ complex range from 2.15 to 2.20 Å, which is peculiar considering that most homoleptic

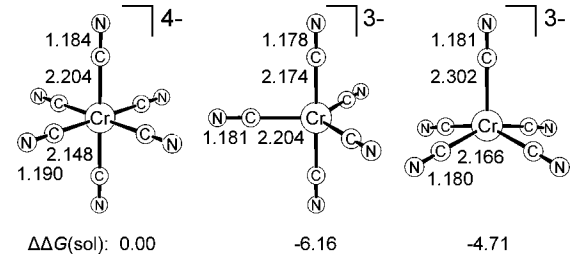

Figure 2. Optimized structures for the low-spin $[Cr(CN)_6]^{4-}$ complex in distorted octahedral (D_{4h}) geometry and the trigonal bipyramidal (D_{3h}) and square pyramidal (C_{4v}) structures for the high-spin $[Cr(CN)_5]^{3-}$ ion. Relative solution phase Gibbs free energies (in acetonitrile) are given in kcal mol^{-1}.

cyano complexes display M−CN bond lengths in the range of 1.9−2.1 Å.[33] Computed Cr−CN bond lengths for the high-spin $[Cr(CN)_5]^{3-}$ complexes vary in the range of 2.17−2.30 Å. These calculations are in good agreement with the experimental work by Nelson et al.,[6] where similarly elongated Cr−CN bond lengths ranging from 2.11 to 2.23 Å in the $(NEt_4)_3[Cr(CN)_5]$ crystal structure were reported.

$[Cr(CN)_6]^{4-}$ versus $[Cr(CN)_5]^{3-}$. Figure 3 shows the electronic energy surface for the loss of a CN^- ligand from the low-spin $[Cr(CN)_6]^{4-}$ ion. The corresponding high-spin energies computed using the same geometries at each point are also shown and illustrate that there is no minimum that could give rise to binding the CN^- ligand on the high-spin energy surface. Whereas there is a minimum for binding the sixth cyanide ligand on the low-spin energy surface, the bonding is very weak, illustrated by the flatness of the low-spin curve, with the depth of the CN^- binding well being 14.4 kcal mol^{-1}. If entropy and solvation corrections are added, the solution-phase free energy of binding becomes only 7 kcal mol^{-1}. The loss of the cyanide ligand from low-spin $[Cr(CN)_6]^{4-}$ to afford the high-spin $[Cr(CN)_5]^{3-}$ complex in trigonal bipyramidal or square pyramidal geometry is thermodynamically favored by 6.2 or 4.7 kcal mol^{-1}, respectively. Although it is impossible to precisely locate the transition states for the loss of one CN^- ligand with standard DFT methods because both entropy and spin-state changes would have to be included, it is safe to take the dissociation limit of 7 kcal mol^{-1} on the low-spin energy surface as an upper limit for the barrier of CN^- loss. Because we are limiting ourselves to a single spin surface to obtain this upper bound, this value should be quite accurate as it is less sensitive to the choice of functional than the values that compare energies for structures on different surfaces. Thus, these calculations suggest that while the low-spin $[Cr(CN)_6]^{4-}$ complex is well-defined in the sense that there is a proper minimum on the potential energy surface, it is highly labile toward lose of a cyanide ligand to afford the thermodynamically more stable high-spin $[Cr(CN)_5]^{3-}$ complex. Even if $[Cr(CN)_6]^{4-}$ were to be formed in solution, it should decompose readily to give the thermodynamically more stable $[Cr(CN)_5]^{3-}$ high-spin complex in the absence of coordinating cations. Deeth previously demonstrated that in

(30) Ziegler, T.; Rauk, A. *Theor. Chim. Acta* **1977**, *46*, 1–10.
(31) Velde, G. T.; Bickelhaupt, F. M.; Baerends, E. J.; Guerra, C. F.; Van Gisbergen, S. J. A.; Snijders, J. G.; Ziegler, T. *J. Comput. Chem.* **2001**, *22*, 931–967.
(32) Albright, T. A.; Burdett, J. K.; Whangbo, M.-H. *Orbital Interactions in Chemistry*; John Wiley & Sons: New York, 1985.
(33) Sharpe, A. G. *The Chemistry of Cyano Complexes of the Transition Metals*; Academic Press Inc.: London, 1976.

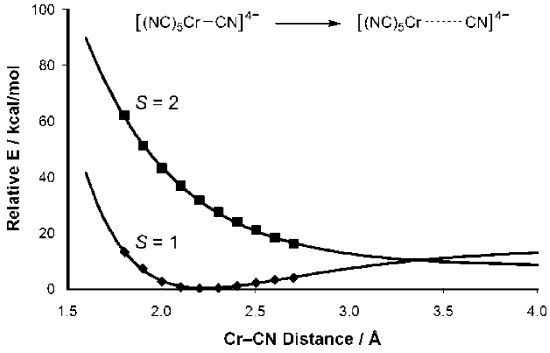

Figure 3. Electronic energy as a function of the Cr−CN distance for both the low- and high-spin configurations of $[Cr(CN)_6]^{4-}$.

more polar media, namely, water, the hexacyano species becomes stable with respect to dissociation.[16] Electrochemical reduction of $[Cr(CN)_6]^{3-}$ to afford $[Cr(CN)_6]^{4-}$ has been studied since the 1940s. Hume and Kolthoff noted that the polarographic reduction wave was poorly defined in the absence of excess KCN, with a brown precipitate being formed.[34] Furthermore, electrolytic reduction showed a second wave with variable height, suggesting that, even in the presence of 1 M KCN, the reduced form is not stable. Replacement of the supporting electrolyte with NaOH led to ECE mechanisms when the sweep rates were sufficiently slow.[35,36] These observations are consistent with a kinetically labile cyanide ligand upon formation of $[Cr(CN)_6]^{4-}$ regardless of the medium used.

A key observation for understanding the bonding in $[Cr(CN)_5]^{3-}$ lies in the unusual Cr−CN bond lengths described above. In addition to the standard σ-donation and π-back-donation, the electrostatic interactions between the metal and the anionic ligands are expected to be important. A plausible hypothesis that would rationalize both the instability of the $[Cr(CN)_6]^{4-}$ ion and the elongated Cr−CN distances in $[Cr(CN)_5]^{3-}$ is that the Cr^{II} center is electrostatically "overloaded". That is, the dicationic chromium center is not able to accommodate six anionic ligands because the Coulombic repulsion between the cyanide ligands is too great without help from coordinating cations. Losing one of the cyanide ligands releases the Coulombic stress affording a stable, five-coordinate species. But even in the five-coordinate complex, Cr^{II} is only able to bind five cyanide ligands by elongating Cr−CN distance beyond the traditional M−CN length to reduce the ligand−ligand Coulombic repulsion. The ligand field strength exerted on a metal center by the coordinated ligands is of course inversely proportional to the M−L distance, that is, the shorter the M−L bond, the larger the energy difference between the low- and high-spin states is expected to be. The attempt to minimize the Coulombic repulsion by elongating the Cr−CN bond leads to weakening of the ligand field because the antibonding overlap between the σ-donor ligand orbitals and the metal e_g orbitals become smaller. As a consequence, the high-spin state that is classically not accessible becomes a feasible alternative.

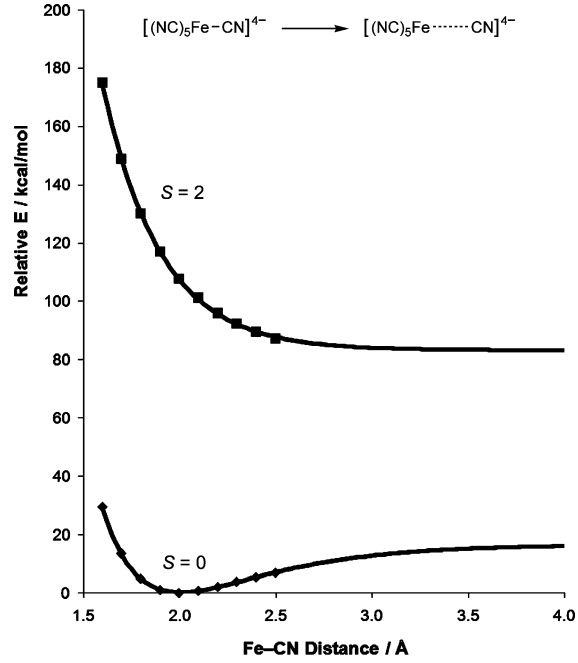

Figure 4. Electronic energy as a function of the Fe−CN distance for both the low- and high-spin configurations of $[Fe(CN)_6]^{4-}$.

If charge overload of a dicationic metal center by six anionic ligands is the dominant feature, it is reasonable that $[Fe^{II}(CN)_6]^{4-}$, another well-known low-spin ($S = 0$) complex as an alkali salt,[33] should also experience a similar force and adopt the unexpected high-spin ($S = 2$) configuration in the presence of noncoordinating cations. A number of Fe^{II} complexes are known and are structurally well characterized in the presence of noncoordinating cations. Representative complexes have classical homoleptic cyano bond lengths close to 1.92 Å.[7−15] These bond lengths are only sensible for the low-spin electronic configuration because the high-spin configuration would place two electrons in strongly antibonding orbitals and thus should result in longer bond lengths, as discussed above for the Cr complex. Our calculated low-spin structure exhibits very similar Fe−CN bond lengths of 1.997 Å. Figure 4 shows a model study on $[Fe(CN)_6]^{4-}$ similar to the one in Figure 3.

As seen for chromium, we found a potential energy surface on the low-spin surface that will give rise to a bound CN^- ligand, whereas the high-spin surface is purely repulsive. However, dramatic differences can be recognized when the two transition metals are compared. First, the depth of the low-spin minimum is substantially greater, and second, the relative spacings between the two surfaces are notably larger for Fe^{II} compared to those for Cr^{II}. Whereas there is a sizable gap of ~35 kcal mol^{-1} for Cr at the optimized low-spin equilibrium geometry, the high- and low-spin curves cross as the Cr−CN distance is increased (Figure 3). The high- and low-spin curves for Fe, on the other hand, are separated by nearly 80 kcal mol^{-1} at the asymptotic limit, disqualifying any spin-crossover that may extrude cyanide in a thermodynamically viable way (Figure 4).

The conceptual frontier orbital picture of octahedral transition-metal complexes (Figure 1a) shows that the t_{2g}

(34) Hume, D. N.; Kolthoff, I. M. *J. Am. Chem. Soc.* **1943**, *65*, 1897–1901.
(35) Jeftic, L.; Feldberg, S. W. *J. Phys. Chem.* **1971**, *75*, 2381.
(36) Feldberg, S. W.; Jeftic, L. *J. Phys. Chem.* **1972**, *76*, 2439.

orbitals are nonbonding while the higher lying e_g orbitals are strongly σ-antibonding along the M−CN vectors. In the presence of strong π-acids, such as cyanide, however, the t_{2g} orbitals become bonding with respect to M−CN by virtue of π-back-donation. The differences in occupation number for the t_{2g} and e_g manifolds have a significant impact on our models. For the low-spin configurations, one expects Fe^{II}-d^6 to be smaller than Cr^{II}-d^4 because of the additional two electrons in the t_{2g} space capable of backbonding. In fact, Fe^{II} has the maximal backbonding capacity for a first-row transition metal. High-spin Fe^{II} on the other hand has two unpaired electrons in the e_g space, compared to only one unpaired electron for Cr^{II}. This observation explains (i) why the M−CN equilibrium distance is shorter for low-spin Fe^{II} and (ii) why the relative energy of the high-spin surface for Fe^{II} is much higher, namely that *two*, instead of *one*, antibonding orbitals are being occupied. The propensity for Fe^{II} to persist as a low-spin hexacyanometallate while Cr^{II} succumbs to charge overload arises from the fine balance between electronics and charge in these systems. This balance can be further dissected using quantitative energy decomposition schemes, as demonstrated in the following section.

High-Spin versus Low-Spin. The observation that the energy difference between the high- and low-spin states becomes smaller because of the charge induced lengthening of the M−L bond described above is easy to understand. A reversal of the energy ordering to give a high-spin complex that is lower in energy than its low-spin analogue at realistic M−L distances, where reasoning based on ligand field theory would predict the latter to be lower in energy, is difficult to understand. The energy components contributing to the total electronic energy can be examined in greater detail by formally reconstructing the molecule from chemically meaningful fragments. In this case, it is most instructive to first place the five cyanide ligands at the coordinates found in the square pyramidal geometry of the chromium complex, as illustrated in eq 6. The energy required to do so is the preparation energy, ΔE_{prep}. Next, Cr^{II} is added, and the interaction energy ΔE_{int} evaluated. The sum of these two energy terms gives the total electronic binding energy ΔE_{bind}, which is directly proportional to the total electronic energy of the complex, and can essentially be used as the electronic energy. Table 1 enumerates the different energy components for both the low-spin (LS) and high-spin (HS) complexes. We also computed the LS and HS energy components of the related complexes $[Cr(CO)_5]^{2+}$ and $[Fe(CN)_5]^{3-}$ for comparison.

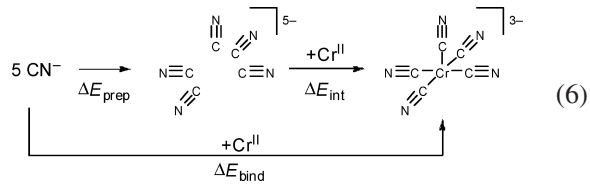

(6)

The computed solution-phase free energy of HS $[Cr(CN)_5]^{3-}$ is 11.6 kcal mol^{-1} lower than that of the LS configuration, in good agreement with the observation that the HS state is the experimentally accessible ground state. Solvation corrections make a notable contribution of 7.5 kcal mol^{-1} in favor of the LS complex, which is easy to understand because more compact structures are expected to expose a higher charge density to solvents. The average Cr−CN distance in the LS complex is 2.087 Å, whereas the HS complex displays an average Cr−CN distance of 2.263 Å (Table 1d). Our calculations show that the HS state is also electronically preferred, illustrated by a ΔE_{bind} that is 16.1 kcal mol^{-1} lower than that of the corresponding LS state (Table 1a). The fragment energy decomposition reveals an interesting and unexpected feature: The electronic interaction between the Cr^{II} center and the preorganized ligand fragments, quantified by ΔE_{int}, is stronger in the LS than in the HS state by 6.4 kcal mol^{-1} (Table 1b), that is, the LS state is favored over the HS state when we only consider the purely electronic component of the M−L interaction, which is in stark contrast to the overall energetic ordering. By examination of the energy components that determine ΔE_{int} in greater detail, this initially puzzling observation becomes plausible: The Pauli repulsion ΔE_{Pauli} favors the HS state by 77.5 kcal mol^{-1}, which reflects the fact that the LS geometry is significantly more compact because the M−L bonds are much shorter than in the HS state ($\Delta = 0.176$ Å). The electron clouds of Cr^{II} and the ligands penetrate to a larger extent, and hence, the Pauli repulsion is larger. For the same reason the electrostatic interaction $\Delta E_{electrostatic}$ favors the LS state by 33.1 kcal mol^{-1} because the anionic charges of the ligands are closer to the cationic charges of the metal center. The partial compensation of higher Pauli penalties by higher electrostatic attraction is an obvious and often observed trend in fragment energy decomposition analyses. Consistent with the intuitive expectation that the M−L orbital interaction should be much stronger in the LS state, our calculations quantify the orbital interaction energy in the LS state to be −518.3 kcal mol^{-1}, whereas only −467.5 kcal mol^{-1} is found in the HS state. This strong orbital interaction term is able to override the greater energy penalty associated with the more compact structure to afford an overall more favorable M−L interaction energy for the LS state.

Thus far, there is nothing special about the M−L interaction in $[Cr(CN)_5]^{3-}$ per se that defies common reasoning based on ligand-field theory as both the energy ordering and energy magnitudes are reasonable, although we note that the energetic difference in orbital interaction between HS and LS states of 50.8 kcal mol^{-1} in the case pentacyanochromate(II) is smaller than one may have expected (vide infra). The key characteristic that makes $[Cr(CN)_5]^{3-}$ special is shown in Table 1c. The assembly of the anionic cyanide ligands into the geometry that they must adopt in the fully optimized pentacyano complex is highly unfavorable because of the Coulombic repulsion that the cyanide ligands exert on each other. The energy penalty of assembling the ligands in the absence of the cationic chromium center, ΔE_{prep}, is not surprisingly much smaller for the less compact HS geometry than the LS analogue. Our calculations quantify this difference to be 22.5 kcal mol^{-1} (Table 1c), thus resulting in the overall interaction energy difference $\Delta\Delta E_{bind}$ of 16.1 kcal mol^{-1} in favor of the HS state.

Table 1. Energy Components of Decomposition Analysis[a]

	$[Cr(CN)_5]^{3-}$ LS	$[Cr(CN)_5]^{3-}$ HS	Δ	$[Cr(CO)_5]^{2+}$ LS	$[Cr(CO)_5]^{2+}$ HS	Δ	$[Fe(CN)_5]^{3-}$ LS	$[Fe(CN)_5]^{3-}$ HS	Δ
				(a) overall energies					
$\Delta E_{bind} = \Delta E_{prep} + \Delta E_{int}$	−630.74	−646.80	−16.06	−305.77	−311.08	−5.31	−677.68	−649.79	27.89
$ZPE - (298\ K)\Delta S$	−10.63	−13.67	−3.04	−12.95	−11.34	1.61	−8.01	−15.29	−7.28
ΔG_{solv}	−357.16	−349.62	7.54	−188.51	−177.59	10.92	−365.73	−347.16	18.57
ΔG(sol)	−988.53	−1010.09	**−11.56**	−507.23	−500.01	**7.57**	−1051.42	−1012.24	**39.34**
				(b) M−L interaction energy components					
ΔE_{Pauli}	302.22	224.75	−77.47	324.89	227.49	−97.40	374.48	137.73	−236.75
$\Delta E_{electrostatic}$	−1168.13	−1135.06	33.07	−173.83	−150.04	23.79	−1225.60	−1112.23	113.37
ΔE_{oi}	−518.31	−467.51	50.80	−474.58	−400.08	74.50	−624.28	−392.40	231.88
ΔE_{int}	−1384.22	−1377.82	**6.40**	−323.52	−322.63	**0.89**	−1475.40	−1366.90	**108.50**
	$[(CN)_5]^{5-}$	$[(CN)_5]^{5-}$	Δ	$(CO)_5$	$(CO)_5$	Δ	$[(CN)_5]^{5-}$	$[(CN)_5]^{5-}$	Δ
				(c) ligand assembly					
ΔE_{Pauli}	43.63	31.46	−12.17	37.35	21.27	−16.08	83.62	23.77	−59.85
$\Delta E_{electrostatic}$	836.35	811.59	−24.76	−6.55	−1.86	4.69	868.31	797.92	−70.39
ΔE_{oi}	−126.50	−112.03	14.47	−13.05	−7.86	5.19	−154.21	−104.58	49.63
ΔE_{prep}	753.48	731.02	**−22.46**	17.75	11.55	**−6.20**	797.72	717.11	**−80.61**
				(d) M−L bond lengths (in Å)					
M−L (av)	2.087	2.263	0.176	2.061	2.163	0.103	1.902	2.198	0.296

[a] In kcal mol^{-1}.

In summary, our analysis identifies the charge of the cyanide ligands that played a key role in determining the instability of the hexacyano complex to again have a dominant effect on the relative energetics of the HS and LS states in the pentacyano complex. We note that the intuitive and common reasoning about the energetics of transition metal complexes based on ligand field theory alone does not take into account the Coulombic stress that charged ligands exert on each other, leading to the expectation that cyanide ligands are without doubt strong-field ligands that should always enforce LS complexes. Our energy decomposition shows that this reasoning is still valid for the pentacyano complex because the M−L interaction is indeed stronger in the LS case, but the Coulombic repulsion caused by the ligand charges reverses this trend in favor of the less compact HS structure. To solidify this conceptual proposal, we also examined the energy components of the related complexes $[Cr(CO)_5]^{2+}$ and $[Fe(CN)_5]^{3-}$. In the former complex, the ligands display similar electronic behavior (σ-donor, π-acceptor, strong-field ligand) but lack the negative charges that we identified to be so important, while in the latter, the charges on the metal center and the ligands are identical to $[Cr(CN)_5]^{3-}$, but there are two additional valence electrons at the iron center to afford a d^6 configuration compared to the d^4 configuration found in the Cr^{II} complex. As mentioned above, both $[Cr(CO)_5]^{2+}$ and $[Fe(CN)_5]^{3-}$ prefer the LS configuration.

Interestingly, the preference of the LS over the HS state is not as pronounced as one may have expected for the $[Cr(CO)_5]^{2+}$ species, with the free energy difference only being in favor of the LS state by 7.6 kcal mol^{-1} (Table 1a). The energy difference is much more decisive for $[Fe(CN)_5]^{3-}$ with the LS state preferred by 39.3 kcal mol^{-1}. As observed before for $[Cr(CN)_5]^{3-}$, solvation energies are notably higher for the LS states with the differential solvation energy being 10.9 and 18.6 kcal mol^{-1} for $[Cr(CO)_5]^{2+}$ and $[Fe(CN)_5]^{3-}$, respectively. The electronic energy ΔE_{bind} indicates that the HS state is preferred for $[Cr(CO)_5]^{2+}$ by 5.3 kcal mol^{-1}, which is surprising and suggests that the charge of the cyanide ligand cannot be the only factor responsible for the unexpected ordering of the spin states. Our calculations indicate that *in the absence of solvation effects, the HS configuration is preferred over the LS analogue even for the pentacarbonyl complex*. A more detailed inspection of the energy components shows that the M−L interaction ΔE_{int} is essentially identical for both spin states with a slight preference of only 0.9 kcal mol^{-1} for the LS configuration (Table 1b). Note that ΔE_{int} showed a preference of 6.4 kcal mol^{-1} for the LS configuration for the pentacyano complex; thus the purely electronic M-L interaction is even more skewed toward the HS configuration in the pentacarbonyl complex.

It is instructive to compare the Pauli repulsion, electrostatic, and orbital interaction components, the sum of which is the M−L interaction energy ΔE_{int}, of the carbonyl and cyano complexes, listed in Table 1b. The Pauli repulsion of 324.9 kcal mol^{-1} between the preorganized carbonyl ligands and the Cr^{II} center is notably higher by nearly 23 kcal mol^{-1} in the LS $[Cr(CO)_5]^{2+}$ complex than in the analogous cyano complex, which can be rationalized by considering that the average Cr−CO distance of 2.061 Å is also notably shorter than 2.087 Å found in the LS $[Cr(CN)_5]^{3-}$ (Table 1d). Because the Pauli repulsion of 227.5 kcal mol^{-1} in the HS carbonyl complex is essentially identical to that found in the HS cyano complex, the differential Pauli repulsion penalty that must be paid to bring the CO ligands in the M−L bonding distance in the LS configuration is 20 kcal mol^{-1} higher in the pentacarbonyl complex than in the pentacyano complex. Because the carbonyl complexes do not carry a charge, the electrostatic M−L interactions are expected to be much smaller, and they are indeed only −173.8 and −150.0 kcal mol^{-1} in the LS and HS configurations, respectively. Lastly, the orbital interaction energy, ΔE_{oi}, strongly favors the LS over the HS complex, with the difference being 74.5 compared to 50.8 kcal mol^{-1} seen for the cyano complex. This is an indication of the stronger

π-back-donation component in the LS carbonyl case compared to the LS cyanide complex because the π^*-orbitals of the carbonyl ligands are lower in energy than those of the cyanides and, thus, are better acceptors. Taken together, these numbers indicate the main reason that the electronic M−L interaction is relatively weak in the LS state of the chromium pentacarbonyl complex is that the Pauli repulsion is relative high and cannot be compensated for fully by the orbital interaction energies.

The ligand assembly energies that were dominated by the electrostatic ligand−ligand repulsions in the cyano-complex are expected to be very small, and our calculations confirm that this is the case. Assembling the CO ligands in the LS geometry only requires 17.8 kcal mol^{-1}, while the HS geometry can be generated with a ΔE_{prep} of only 11.6 kcal mol^{-1}. Note that these energy penalties were 753.5 and 731.0 kcal mol^{-1} in the low- and high-spin cyano complexes, respectively. The addition of this differential energy that favors the less compact geometry of the HS complex, and the overall binding energy is in slight preference of the HS complex. In conclusion, the trends found in the M−L interaction energies of the chromium carbonyl complexes are unexpected at first, but the energy components are reasonable when examined separately. Our analysis is still not satisfying, however, because it does not provide an intuitively comprehensible answer to the following fundamental question: What makes the Cr^{II}−penta(cyanide/carbonyl) complexes so unusual that the HS and LS states are energetically so close to each other that solvation effects and charge-induced lengthening of the M−L bonds, which may be considered secondary effects, are enough to reverse the relative energy ordering of the high- and low-spin states?

The pentacyanoferrate(II) complex provides a convenient benchmark for gauging the magnitudes of the different energy components. As mentioned above, the solution-phase free-energy difference between the LS and HS configurations of $[Fe(CN)_5]^{3-}$ is 39.3 kcal mol^{-1} in favor of the LS state. The electronic portion of this energy gap expressed in ΔE_{bind} is 27.9 kcal mol^{-1} (Table 1a). Among the complexes discussed so far, the LS $[Fe(CN)_5]^{3-}$ adopts the most compact geometry with the shortest average M−CN bond length of 1.902 Å, and thus, the ligand assembly is most unfavorable with a ΔE_{prep} value of 797.7 kcal mol^{-1}. Because the HS analogue displays an elongated M−CN bond length of 2.198 Å, the difference $\Delta\Delta E_{prep}$ is very large at 80.6 kcal mol^{-1} in favor of the HS complex, reflecting on the large M−CN bond length difference of nearly 0.3 Å between LS $[Fe(CN)_5]^{3-}$ and its putative HS analogue. Interestingly, the ΔE_{int} is similarly large and favors the LS state by 108.5 kcal mol^{-1}. The components of ΔE_{int} are very useful to compare to the chromium systems. The Pauli repulsion is highly in favor of the HS state, as we have seen before and are counterbalanced by the electrostatic component somewhat. A comparison of $\Delta\Delta E_{Pauli}$ and $\Delta\Delta E_{electrostatic}$ of −236.7 and 113.4 kcal mol^{-1}, respectively, to the values seen in the chromium analogue (−77.5 and 33.1 kcal mol^{-1}) and consideration of the structural differences between the HS and LS states, which are more pronounced in the iron complex, shows that the sum of these two differential energy terms of −123.4 and −43.9 kcal mol^{-1} is plausible.

What is perhaps most surprising is the enormous difference in the orbital interaction term. In the iron system, $\Delta\Delta E_{oi}$ is 231.9 kcal mol^{-1}, which is almost five times greater than the orbital interaction energy difference of 50.8 kcal mol^{-1} between the HS and LS states that was seen for chromium. This preference in orbital interaction energy can easily override the energetic discrimination of the LS state on the basis of Pauli repulsion originating from the more compact geometry. The reason for the stronger orbital interaction component becomes obvious when we consider that the low-spin Fe^{II}-d^6 center is a much better π-back-donor than a low-spin Cr^{II}-d^4 center, which is the reason that the Fe−CN bond is so short compared to the chromium complexes, as well as the fact that two electrons are placed in the energetically unfavorable M−L antibonding orbitals in the HS configuration. This affords the Fe^{II}-d^6 complex with a higher degree of destabilization compared to the Cr^{II}-d^4 system, where only one electron is placed in the M−L antibonding manifold.

This insight highlights what is required for a transition metal complex with strong field ligands to display the classical spin state energy ordering: The M−L orbital interaction energy in the LS complex must be sufficiently large to override both the Pauli repulsion and ligand assembly energies that will always disfavor the structurally more compact LS states. One way of doing so is to use the π-back-donation, which will be strongest in d^6 systems. The Cr(II) complexes discussed above possess d^4 centers that are weak low-spin π-donors, where only one of the metal-d-orbitals is doubly occupied. In addition, only one M−L antibonding orbital is occupied in the HS state of the d^4 system, causing the HS state to be relatively low in energy. In combination, these effects afford a very small energy gap between the HS and LS states of the $[Cr(CN)_5]^{3-}$ complex. Consequently, small structural changes, such as M−L bond length changes caused by "charge-overload", described in detail above, or environmental effects, such as solvation, can easily tip the energetic balance one or the other way.

Conclusions

We examined the curious experimental observation that the homoleptic hexacyanochromate(II) complex anion appears to be thermodynamically unstable in acetonitrile when no coordinating cations are present. The resulting pentacyano complex was found to display a high-spin configuration in its ground state. This finding was puzzling because a low-spin state is intuitively expected for the Cr^{II}-d^4-system on the basis of ligand field theory considerations because cyanide ligands are widely recognized to give very strong ligand fields. Utilizing a fragment energy decomposition scheme to understand the M−L interactions, we found that the relative magnitude of the purely electronic component is in good agreement with intuitive expectations, that is, the orbital interaction energy is larger in low-spin $[Cr(CN)_5]^{3-}$ than in its high-spin analogue. This electronic preference of the low-spin state is overridden, however, by the higher Coulombic repulsion that must be overcome when forcing

the anionic cyanide ligands into the more compact geometry required for the low-spin pentacyano complex. To generalize the interaction patterns that we described for the $[Cr(CN)_5]^{3-}$complex anion, we carried out analogous analyses for
$[Cr(CO)_5]^{2+}$ and $[Fe(CN)_5]^{3-}$. By comparing the chromium and iron analogues, we were able to better conceptualize the electronic features that lead to the unusual spin-state energy ordering of the chromium complex. The combination of poor π-back-donation ability of the low-spin Cr^{II}-d^4-center giving rise to a relatively high-energy low-spin state and the placement of only a single electron in the M−L antibonding orbital in the high-spin configuration, resulting in a relatively low-energy high-spin state, brings the spin surfaces remarkably close to one another. Small changes in M−L bond lengths caused by Coulombic ligand−ligand repulsions are sufficient in this scenario to push the low-spin state higher in energy than the high-spin state.

Acknowledgment. We thank the NSF (CHE-0645381 and 0116050 to Indiana University) for financial support. M.H.B. is a Cottrell scholar of the Research Corporation and an Alfred P. Sloan fellow of the Alfred P. Sloan Foundation. R.L.L. thanks the Merck Research Corporation for a graduate fellowship and the Department of Education for a GAANN fellowship, and William H. Pitcock Jr. and Franklin A. Schultz for helpful discussions.

Supporting Information Available: Computational details, Cartesian coordinates, and detailed energies. This material is available free of charge via the Internet at http://pubs.acs.org.

IC8000653